ACADÉMIE
DES SCIENCES
INSTITUT DE FRANCE

Comptes Rendus
Physique

Guillaume Michel

Coupled dynamics of a wave and moving boundary

Volume 26 (2025), p. 259-270

Online since: 5 March 2025

https://doi.org/10.5802/crphys.242

The Comptes Rendus. Physique *are a member of the Mersenne Center for open scientific publishing*
www.centre-mersenne.org — e-ISSN : 1878-1535

ACADÉMIE DES SCIENCES
INSTITUT DE FRANCE

Comptes Rendus. Physique
2025, Vol. 26, p. 259-270
https://doi.org/10.5802/crphys.242

Research article / *Article de recherche*

Coupled dynamics of a wave and moving boundary

Dynamique couplée d'une onde et d'une paroi mobile

Guillaume Michel [a]

[a] Sorbonne Université, CNRS, Institut Jean Le Rond d'Alembert, F-75005 Paris, France
E-mail: guillaume.michel@sorbonne-universite.fr

Abstract. I present the dynamics of waves trapped in a one-dimensional cavity with a single wall that can move as a result of radiation pressure (and possibly other external forces). Specifically, the classical wave equation is considered and the phenomenology of this system is outlined when the moving boundary achieves large displacements and velocities similar to the one of the waves. Governing equations are derived in the context of electromagnetism, and a spatial discretization that conserves the total energy is proposed. I address cases when the dynamics of the boundary are prescribed or critically damped. Finally, numerical simulations are performed to obtain qualitative results for the conservative limit.

Résumé. Je présente la dynamique d'ondes dans une cavité unidimensionnelle dont une paroi peut se mettre en mouvement sous l'effet, entre autres, de la pression de radiation. Plus précisément, l'équation des ondes classiques est couplée à une paroi subissant de grands déplacements et pouvant se mouvoir à une vitesse comparable à celle des ondes. Les équations du problème sont obtenues dans le cadre de l'électromagnétisme puis discrétisées spatialement en conservant l'énergie totale. Quelques cas particuliers sont ensuite traités, lorsque la position de la paroi est prescrite par un opérateur extérieur ou bien se réduit à un oscillateur dans son régime critique. Des simulations numériques dans la limite conservatives sont finalement discutées.

Keywords. Wave, Radiation pressure, Moving boundary, Nonlinear dynamics, Doppler effect.

Mots-clés. Ondes, Pression de radiation, Paroi mobile, Dynamique non linéaire, Effet Doppler.

Note. Guillaume Michel is the 2024 recipient of the Jacques Herbrand/Fondation Mireille Cahn-Bunel prize of the Académie des Sciences.

Manuscript received 25 November 2024, revised 12 February 2025, accepted 24 February 2025.

1. Introduction

The Doppler effect constitutes a canonical example of an interaction between a wave and a moving boundary: traveling solutions of the wave equation present changes in both their energy and frequency as they reflect off a uniformly moving boundary [1]. This result has been widely generalized to non-uniform motions. For instance, quasi-monochromatic waves of frequency f_0 reflecting off a harmonically oscillating boundary at frequency f_b acquire a spectrum of the form $\{f_0 + nf_b\}_{n\in\mathbb{Z}}$ that can be explicitly computed [2]. This holds for electromagnetic waves and—after much controversy over the comparative effects of the medium non-linearity [3]—has also been experimentally confirmed for acoustic waves [4]. This approach can be adapted for surface gravity waves, even though they are not governed by the standard wave equation [5].

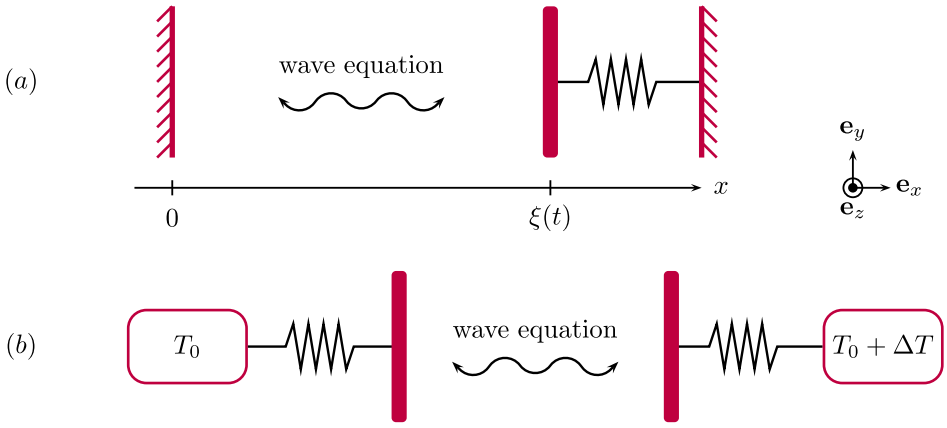

Figure 1. Two examples of one-dimensional wave fields coupled with moving boundaries. (a) A model that allows energy conservation and investigation into the characteristics of the stationary state. (b) A model of heat transfer mediated by radiation pressure (i.e., caused neither by conduction or convection nor by emission or absorption of radiation).

A natural extension of these works is to consider the cumulative effects of such generalized Doppler shifts for waves trapped in a cavity with oscillating walls. The one-dimensional wave equation in the modulated domain $[0, L_0 + A\cos(2\pi f_b t)]$ with non-zero initial conditions leads, in some range of parameters, to a localization and exponential growth in wave energy [6,7]. This parametric instability is known as the dynamical Casimir effect in quantum electrodynamics and can generate photons in a vacuum [8]. This instability is also considered in the construction of ultra-short pulses [9] and contributes to the interpretations of experiments on wave turbulence [5]. In practice, the motion of the oscillating wall becomes increasingly difficult to sustain as the wave energy continues to grow.

In the problems discussed above, the position of the moving boundary is assumed to be prescribed regardless of the radiation pressure generated by the waves. Taking this feedback into account enables a large class of new phenomena related to thermalization and heat fluxes to be investigated. Consider, for instance, the setup shown in Figure 1(a), in which a wave propagates in a cavity whose right wall is connected to a spring. The energy of this entire system is conserved, but does it eventually thermalize? And how long does it take? Similar questions arise if two of these moving boundaries are now introduced (the left and right walls), and connected to thermostats of different temperatures, see Figure 1(b). Is there a mean heat flux in this system? If yes, how does it scale with the temperature difference? Does it depend on the initial wave energy?

As a result of the tremendous potential applications of optomechanics [10,11], the modeling of such systems, initially based on the classical wave equation, nowadays involves quantized electromagnetic fields and boundary motions [12]. The framework developed by Law [13] is routinely used (see, e.g., [14–16] and references therein). It crucially relies on both nonrelativistic and small-displacements assumptions; in addition, most studies restrict to a few electromagnetic modes (generally a single one). In contrast, I focus in this manuscript on the opposite limit of cavities driven by radiation pressure in which a large number of wave modes interact with a boundary that undergoes large displacements and can move up to the speed of the waves. I try to provide here a pedagogical introduction to the governing equations and emerging properties as well as a simple numerical scheme able to capture this complex dynamics. Classical electromagnetism is used for that purpose, but the general picture is expected to hold for mechanical waves as well.

The remainder of this manuscript is organized as follows. The radiation pressure is derived from the wave equation in Section 2. I introduce in Section 3 the governing equations of the problem displayed in Figure 1(a) ((b) being an immediate extension) and propose an energy-conserving discretization in Section 4. I then discuss a few cases in which theoretical predictions can be drawn in Section 5 and investigate the fully conservative limit using numerical simulations in Section 6.

2. The radiation pressure and the wave equation

The investigation of the coupling between a wave field and a moving boundary requires an expression for the radiation pressure. There is a simple way to derive its expression: it is reported here as, in my opinion, one of the most straightforward introduction to radiation pressure that can be done in classroom. Consider the wave equation for a field $A(x,t)$ in the domain $x \in [0, \xi(t)]$ with Dirichlet boundary conditions,

$$\frac{\partial^2 A}{\partial t^2} = c^2 \frac{\partial^2 A}{\partial x^2}, \quad A[0,t] = A[\xi(t),t] = 0, \tag{1}$$

and the energy associated with this field (up to a dimensional constant),

$$E_{\text{waves}}(t) = \int_0^{\xi(t)} \left[\frac{1}{2} \left(\frac{\partial A}{\partial x} \right)^2 + \frac{1}{2c^2} \left(\frac{\partial A}{\partial t} \right)^2 \right] \mathrm{d}x. \tag{2}$$

The time derivative of this energy is computed as

$$\frac{\mathrm{d}E_{\text{waves}}}{\mathrm{d}t} = \int_0^{\xi(t)} \left[\frac{\partial A}{\partial x} \frac{\partial^2 A}{\partial x \partial t} + \frac{1}{c^2} \frac{\partial A}{\partial t} \frac{\partial^2 A}{\partial t^2} \right] \mathrm{d}x + \dot{\xi} \left[\frac{1}{2} \left(\frac{\partial A}{\partial x} \right)^2 [\xi(t),t] + \frac{1}{2c^2} \left(\frac{\partial A}{\partial t} \right)^2 [\xi(t),t] \right]. \tag{3}$$

The integral can be computed using integration by part, the wave equation and the boundary condition at $x = 0$, $A[0,t] = 0 \rightarrow \partial_t A[0,t] = 0$.

$$\int_0^{\xi(t)} \left[\frac{\partial A}{\partial x} \frac{\partial^2 A}{\partial x \partial t} + \frac{1}{c^2} \frac{\partial A}{\partial t} \frac{\partial^2 A}{\partial t^2} \right] \mathrm{d}x = \int_0^{\xi(t)} \left[\frac{\partial A}{\partial t} \left(\frac{1}{c^2} \frac{\partial^2 A}{\partial t^2} - \frac{\partial^2 A}{\partial x^2} \right) \right] \mathrm{d}x + \left[\frac{\partial A}{\partial t} \frac{\partial A}{\partial x} \right]_0^{\xi(t)} \tag{4}$$

$$= \left(\frac{\partial A}{\partial t} \right) [\xi(t),t] \left(\frac{\partial A}{\partial x} \right) [\xi(t),t]. \tag{5}$$

Finally, the second boundary condition results in $A[\xi(t),t] = 0 \rightarrow \partial_t A[\xi(t),t] = -\dot{\xi} \partial_x A[\xi(t),t]$ and this energy budget reveals the expression of the power generated by the moving boundary,

$$\frac{\mathrm{d}E_{\text{waves}}}{\mathrm{d}t} = \left(\frac{\partial A}{\partial t} \right) [\xi(t),t] \left(\frac{\partial A}{\partial x} \right) [\xi(t),t] + \dot{\xi} \left[\frac{1}{2} \left(\frac{\partial A}{\partial x} \right)^2 [\xi(t),t] + \frac{1}{2c^2} \left(\frac{\partial A}{\partial t} \right)^2 [\xi(t),t] \right] \tag{6}$$

$$= -\dot{\xi} \frac{(\partial_x A)^2 [\xi(t),t]}{2} \left(1 - \frac{\dot{\xi}^2}{c^2} \right) \equiv -\dot{\xi} P_{\text{rad}}, \tag{7}$$

hence the expression for the radiation pressure P_{rad} (up to the dimensional constant of (2)). If A is the electromagnetic vector potential, this yields the relativistic radiation pressure on a moving perfect mirror that will be considered Section 3.3, but it also applies to simpler mechanical systems such that vibrating strings of variable lengths.

3. Governing equations

The considered model is presented in Figure 1(a). It consists of waves in a one-dimensional cavity whose left wall is fixed and whose right wall is free to respond to the radiation pressure and other external forces. Even though this setup is generic, it will be described for the specific framework of electromagnetism in a vacuum, with the walls assumed to be massive perfect mirrors. The main reasons guiding this choice are that (i) the wave dynamics in the cavity are

fully linear, (ii) the motion of a mirror does not directly generate waves, and (iii) the velocity of the massive mechanically moving wall cannot exceed the wave speed. These stipulations would not hold for acoustic or surface waves. In this section, different equivalent sets of equations will be introduced, some useful for concise analytic predictions and others for simple numerical implementation.

3.1. *In terms of the dimensional electromagnetic fields*

Let x denote the spatial coordinate: the positions of the mirrors are 0 (left, fixed wall) and $\xi(t)$ (right, moving wall). A single linear polarization is considered, corresponding to an electric field $\mathbf{E}(x,t) = E(x,t)\mathbf{e}_y$ and magnetic field $\mathbf{B}(x,t) = B(x,t)\mathbf{e}_z$. The propagation and radiation force of these fields depend on the magnetic permeability of free space μ_0 and the speed of light c. The moving boundary is subject to the electromagnetic radiation pressure, a linear restoring force, and potentially other external forces and is therefore characterized, per unit surface, by its mass M_s, its spring constant K_s (of rest position L_0), and additional forces $\mathbf{F}_{\text{ext}} = F_{\text{ext}}\mathbf{e}_x$. The governing equations are thus:

$$\frac{\partial E}{\partial x} = -\frac{\partial B}{\partial t}, \quad \frac{\partial E}{\partial t} = -c^2\frac{\partial B}{\partial x}, \quad E[0,t] = 0, \quad E[\xi(t),t] = \dot{\xi}B[\xi(t),t], \tag{8}$$

$$M_s\frac{\mathrm{d}}{\mathrm{d}t}\left(\gamma\dot{\xi}\right) = -K_s(\xi - L_0) + F_{\text{ext}} + \frac{B[\xi(t),t]^2}{2\mu_0}\left(1 - \frac{\dot{\xi}^2}{c^2}\right), \quad \gamma = \left(1 - \frac{\dot{\xi}^2}{c^2}\right)^{-1/2}. \tag{9}$$

The boundary conditions (8) set the electric field to zero at the perfect mirrors in their frames of reference. The relativistic dynamics (9) prevent the velocity of the boundary from reaching c. These equations conserve the total energy in the absence of external forces,

$$\frac{\mathrm{d}}{\mathrm{d}t}\left[M_s\gamma c^2 + K_s\frac{(\xi - L_0)^2}{2} + \int_0^\xi\left(\frac{E^2}{2\mu_0 c^2} + \frac{B^2}{2\mu_0}\right)\mathrm{d}x\right] = \dot{\xi}F_{\text{ext}}. \tag{10}$$

3.2. *In terms of the dimensionless electromagnetic fields*

The dimensionless fields and variables are defined as

$$x = L_0\bar{x}, \quad t = (L_0/c)\bar{t}, \quad \xi(t) = L_0\bar{\xi}(\bar{t}), \tag{11}$$

$$B(x,t) = \sqrt{\mu_0 K_s L_0}\bar{B}(\bar{x},\bar{t}), \quad E(x,t) = c\sqrt{\mu_0 K_s L_0}\bar{E}(\bar{x},\bar{t}), \quad F_{\text{ext}} = K_s L_0\bar{F}_{\text{ext}}. \tag{12}$$

They will be considered throughout the remainder of this manuscript; therefore, I have omitted the over-bars in subsequent equations. The governing equations and energy budget become

$$\frac{\partial E}{\partial x} = -\frac{\partial B}{\partial t}, \quad \frac{\partial E}{\partial t} = -\frac{\partial B}{\partial x}, \quad E[0,t] = 0, \quad E[\xi(t),t] = \dot{\xi}B[\xi(t),t] \tag{13}$$

$$\alpha^2\frac{\mathrm{d}}{\mathrm{d}t}\left(\gamma\dot{\xi}\right) = 1 - \xi + F_{\text{ext}} + \frac{B[\xi(t),t]^2}{2}\left(1 - \dot{\xi}^2\right), \quad \gamma = \left(1 - \dot{\xi}^2\right)^{-1/2}, \tag{14}$$

$$\frac{\mathrm{d}}{\mathrm{d}t}\left[\alpha^2\gamma + \frac{(\xi - 1)^2}{2} + \int_0^\xi\left(\frac{E^2}{2} + \frac{B^2}{2}\right)\mathrm{d}x\right] = \dot{\xi}F_{\text{ext}}, \tag{15}$$

where $\alpha = c/(L_0\omega)$ and $\omega = \sqrt{K_s/M_s}$ the natural angular frequency of the boundary.

3.3. *In terms of the dimensionless vector potential*

The theoretical analysis of this system, especially when the motion of the boundary is prescribed, is facilitated by the introduction of the dimensionless vector potential A (specifically its y-component) such that $B = \partial_x A$ and $E = -\partial_t A$. The governing equations are:

$$\frac{\partial^2 A}{\partial x^2} = \frac{\partial^2 A}{\partial t^2}, \quad A[0,t] = A[\xi(t),t] = 0, \quad \alpha^2\frac{\mathrm{d}}{\mathrm{d}t}\left(\gamma\dot{\xi}\right) = 1 - \xi + F_{\text{ext}} + \frac{(\partial_x A)[\xi(t),t]^2}{2}\left(1 - \dot{\xi}^2\right). \tag{16}$$

3.4. *In terms of the dimensionless energy density and flux*

These equations can be expressed in terms of the energy density $u = (E^2 + B^2)/2$ and flux $P = EB$:

$$\frac{\partial u}{\partial t} = -\frac{\partial P}{\partial x}, \quad \frac{\partial P}{\partial t} = -\frac{\partial u}{\partial x}, \quad P[0,t] = 0, \quad P[\xi,t] = \frac{2\dot{\xi}\,u[\xi(t),t]}{1+\dot{\xi}^2}, \tag{17}$$

$$\alpha^2 \frac{\mathrm{d}}{\mathrm{d}t}\left(\gamma\dot{\xi}\right) = 1 - \xi + F_{\mathrm{ext}} + u[\xi(t),t]\left(\frac{1-\dot{\xi}^2}{1+\dot{\xi}^2}\right). \tag{18}$$

The electromagnetic energy no longer involves squared fields and is given by $E_{\mathrm{em}} = \int_0^\xi u(x,t)\,\mathrm{d}x$.

4. Numerical model

Numerical discretization of these equations can be achieved using finite-difference time-domain (FDTD) on a fixed grid by choosing adequate boundary conditions and adding and removing grid points as the boundary moves [17,18]. In this study, I used the more direct approach of introducing stretched coordinates on which the governing equations are discretized; thus, the cavity is always represented by a constant number of grid points. This method requires no alteration to the boundary conditions and makes energy conservation straightforward. However, contrary to FDTD, it cannot generalize to higher spatial dimensions.

4.1. *Governing equations in the stretched domain*

The introduction of the stretched coordinates $(\tilde{t},\tilde{x}) = (t, x/\xi(t))$ makes the domain size constant, that is, $x \in [0,\xi(t)] \to \tilde{x} \in [0,1]$. Further, the partial derivatives of any field $f(x,t) = \tilde{f}(\tilde{x},\tilde{t})$ are easily related:

$$\left(\frac{\partial f}{\partial x}\right)_t = \frac{1}{\xi}\left(\frac{\partial \tilde{f}}{\partial \tilde{x}}\right)_{\tilde{t}}, \quad \left(\frac{\partial f}{\partial t}\right)_x = \left(\frac{\partial \tilde{f}}{\partial \tilde{t}}\right)_{\tilde{x}} - \frac{\tilde{x}\dot{\xi}}{\xi}\left(\frac{\partial \tilde{f}}{\partial \tilde{x}}\right)_{\tilde{t}}. \tag{19}$$

The governing equations reported in Section 3.4 and the energy budget become

$$\frac{\partial \tilde{u}}{\partial \tilde{t}} = -\frac{1}{\xi}\frac{\partial \tilde{P}}{\partial \tilde{x}} + \frac{\tilde{x}\dot{\xi}}{\xi}\frac{\partial \tilde{u}}{\partial \tilde{x}}, \quad \frac{\partial \tilde{P}}{\partial \tilde{t}} = -\frac{1}{\xi}\frac{\partial \tilde{u}}{\partial \tilde{x}} + \frac{\tilde{x}\dot{\xi}}{\xi}\frac{\partial \tilde{P}}{\partial \tilde{x}}, \quad \tilde{P}[0,\tilde{t}] = 0, \quad \tilde{P}[1,\tilde{t}] = \frac{2\dot{\xi}\,\tilde{u}[1,\tilde{t}]}{1+\dot{\xi}^2}, \tag{20}$$

$$\alpha^2 \frac{\mathrm{d}}{\mathrm{d}\tilde{t}}\left(\gamma\dot{\xi}\right) = 1 - \xi + F_{\mathrm{ext}} + \tilde{u}[1,\tilde{t}]\left(\frac{1-\dot{\xi}^2}{1+\dot{\xi}^2}\right), \quad \frac{\mathrm{d}}{\mathrm{d}\tilde{t}}\left[\alpha^2\gamma + \frac{(\xi-1)^2}{2} + \xi\int_0^1 \tilde{u}(\tilde{x},\tilde{t})\,\mathrm{d}\tilde{x}\right] = \dot{\xi}F_{\mathrm{ext}}. \tag{21}$$

4.2. *Spatiotemporal discretization*

These equations are then discretized in space with staggered finite-difference grids. The discretized energy fluxes $\{\tilde{P}_n\}_{n\in[0,N]}$ relate to the spatial positions $\{\tilde{x}_n = n\Delta X\}_{n\in[0,N]}$ with $\Delta X = 1/N$, whereas the mesh for the energy densities $\{\tilde{u}_{n+1/2}\}_{n\in[-1,N]}$ lies at $\{\tilde{x}_{n+1/2} = (n+1/2)\Delta X\}_{n\in[-1,N]}$. The derivatives are approximated as

$$\frac{\partial \tilde{u}_{n+1/2}}{\partial \tilde{t}} = -\frac{1}{\xi}\left(\frac{\tilde{P}_{n+1} - \tilde{P}_n}{\Delta X}\right) + \left(\frac{\tilde{x}_{n+1/2}\dot{\xi}}{\xi}\right)\left(\frac{\tilde{u}_{n+3/2} - \tilde{u}_{n-1/2}}{2\Delta X}\right), \quad n \in [0, N-1] \tag{22}$$

$$\frac{\partial \tilde{P}_n}{\partial \tilde{t}} = -\frac{1}{\xi}\left(\frac{\tilde{u}_{n+1/2} - \tilde{u}_{n-1/2}}{\Delta X}\right) + \left(\frac{\tilde{x}_n\dot{\xi}}{\xi}\right)\left(\frac{\tilde{P}_{n+1} - \tilde{P}_{n-1}}{2\Delta X}\right), \quad n \in [1, N-1] \tag{23}$$

$$\tilde{P}_0 = 0, \quad \tilde{P}_N = \frac{\dot{\xi}(\tilde{u}_{N-1/2} + \tilde{u}_{N+1/2})}{1+\dot{\xi}^2}, \quad \alpha^2\frac{\mathrm{d}}{\mathrm{d}\tilde{t}}\left(\gamma\dot{\xi}\right) = 1 - \xi + F_{\mathrm{ext}} + \frac{(\tilde{u}_{N-1/2} + \tilde{u}_{N+1/2})}{2}\left(\frac{1-\dot{\xi}^2}{1+\dot{\xi}^2}\right). \tag{24}$$

Prescribing the ghost nodes $\tilde{u}_{-1/2} = \tilde{u}_{1/2}$ and $\tilde{u}_{N+1/2} = \tilde{u}_{N-1/2}$ enforces the discrete energy budget,

$$\frac{\mathrm{d}}{\mathrm{d}\tilde{t}}\left[\alpha^2\gamma + \frac{(\xi-1)^2}{2} + \xi \sum_{n\in[0,N-1]} \tilde{u}_{n+1/2}\Delta X\right] = \dot{\xi}F_{\mathrm{ext}}. \tag{25}$$

Notably, although this spatial discretization conserves the total energy, the propagation becomes dispersive and the energy density is no longer guarantied to remain positive (these features become more apparent with energy variations at small scales $O(\Delta X)$). Finally, Equations (22)–(24) are numerically implemented and advanced in time using a fourth-order Runge–Kutta scheme. All the simulations reported in this article were performed with $N = 10^5$ grid points, unless stated otherwise, and a fixed timestep $\Delta t = 1/(2N)$.

5. Limit cases

5.1. *Waves in a harmonically modulated cavity*

Here, a few simple cases will be illustrated using the numerical model. The first considers the canonical problem of waves in a cavity of harmonically modulated length. It is mainly presented as an introduction to the phenomenology of waves in a modulated domain but also serves as a test case for our numerical method and as an introduction to the theoretical recurrence relations.

5.1.1. *Recurrence relations*

Recurrence relations can be derived from the vector potential equations obtained in Section 3.3. They characterize the back-and-forth propagation of waves in the cavity, along with their change in amplitude as they reflect off the moving boundary. The general solution of the wave equation (16) is

$$A(x,t) = A_+(x+t) + A_-(x-t). \tag{26}$$

The boundary conditions are enforced with these new functions, then differentiated with time:

$$A[\xi(t),t] = 0 = A_+[\xi(t)+t] + A_-[\xi(t)-t] \quad \Longrightarrow \dot{A}_+[\xi(t)+t] = \left(\frac{1-\dot{\xi}(t)}{1+\dot{\xi}(t)}\right)\dot{A}_-[\xi(t)-t], \tag{27}$$

$$A(0,t) = 0 = A_+(t) + A_-(-t) \Longrightarrow \dot{A}_+(t) = \dot{A}_-(-t) \quad \Longrightarrow \partial_x A(0,t) = 2\dot{A}_+(t) = 2\dot{A}_-(-t). \tag{28}$$

Since t is arbitrary in (28), this results in both

$$\partial_x A[0, t+\xi(t)] = 2\dot{A}_+[t+\xi(t)], \quad \partial_x A[0,t-\xi(t)] = 2\dot{A}_-[\xi(t)-t]. \tag{29}$$

Combining (27) and (29) gives

$$\partial_x A[0,t+\xi(t)] = \left(\frac{1-\dot{\xi}(t)}{1+\dot{\xi}(t)}\right)\partial_x A[0,t-\xi(t)]. \tag{30}$$

Equation (30) provides a relation between the fields at the left (stationnary) boundary before $(t-\xi(t))$ and after $(t+\xi(t))$ they reflect off the moving mirror (at time t). This equation is well-known and can be found in several instances in the literature (Equations (7) and (8) in Ref. [7]). To express this result in terms of the variables used in our numerical formulation, I introduce the radiation pressure $\mathscr{P}$ acting on the moving boundary and the energy density u_L measured on the left boundary from (16):

$$\mathscr{P}(t) = \frac{\partial_x A[\xi(t),t]^2}{2}(1-\xi(t)^2), \quad u_L(t\pm\xi(t)) = \frac{\partial_x A[0,t\pm\xi(t)]^2}{2}. \tag{31}$$

Differentiating (26) with respect to x and then (29) and (30), I obtain

$$\partial_x A\left[\xi(t),t\right]=\dot{A}_+\left[\xi(t)+t\right]+\dot{A}_-\left[\xi(t)-t\right]=\frac{\partial_x A\left[0,t+\xi(t)\right]+\partial_x A\left[0,t-\xi(t)\right]}{2}=\frac{\partial_x A\left[0,t-\xi(t)\right]}{1+\dot{\xi}(t)}. \tag{32}$$

Finally, recurrence relations on both u_L and $\mathscr{P}$ are

$$\mathscr{P}(t)=\left(\frac{1-\dot{\xi}(t)}{1+\dot{\xi}(t)}\right)u_L\left[t-\xi(t)\right],\quad u_L\left[t+\xi(t)\right]=\left(\frac{1-\dot{\xi}(t)}{1+\dot{\xi}(t)}\right)^2 u_L\left[t-\xi(t)\right]. \tag{33}$$

These hold irrespective of the specific motion of the boundary $\xi(t)$. They track the propagation of the energy density at the left wall at time $t-\xi(t)$ such that they relate (i) to the radiation pressure generated at time t when the wave meets the mirror with position $\xi(t)$, and (ii) to the new energy density modified by Doppler effect that returns to the left wall at time $t+\xi(t)$.

5.1.2. *Divergence of the energy at $\omega\simeq c\pi/L_0$*

Assume that an external force drives the left boundary according to $\xi(t)=L_0\left[1+a\sin(\omega t)\right]$, i.e., that with dimensionless variables $\xi(t)=1+a\sin(\alpha^{-1}t)$ ($0<a<1$ and $a<\alpha$). Thus, if $\alpha^{-1}=\pi$, that is, if $\omega=c\pi/L_0$ is the first non-zero eigenfrequency of the electromagnetic cavity at rest, the recurrence relation (33) for u_L at times $t_n=2n$ (such that $\xi(t_n)=1$ and $\xi'(t_n)=a\pi$) becomes

$$u_L(2n+1)=\left(\frac{1+a\pi}{1-a\pi}\right)^2 u_L(2n-1)=\left(\frac{1+a\pi}{1-a\pi}\right)^4 u_L(2n-3)=\cdots=\left(\frac{1+a\pi}{1-a\pi}\right)^{2n} u_L(1), \tag{34}$$

representing energy divergence. The same procedure can be adapted for an α^{-1} that slightly differs from π. This divergence persists in the range [6]

$$\frac{\omega L_0}{c}\in\left[\frac{\pi}{1+a},\frac{\pi}{1-a}\right]. \tag{35}$$

Numerical simulations were performed with the same initial conditions and boundary motion as in Ref. [6]: $u(x,0)=P(x,0)=\exp[-60(x-0.5)^2]$ and $\xi(t)=1+a\sin(\alpha^{-1}t)$ with $a=0.2$. I refer the reader to the additional movies Movie_inva2 ($\alpha^{-1}=2$) and Movie_inva3 ($\alpha^{-1}=3$) (Supplementary information). The second movie clearly depicts cumulative Doppler effects that dramatically increase the energy of a pulse propagating back and forth. The energy of the waves as a function of α^{-1} and t is shown in Figure 2(left); it reproduces the instability range of (35) and coincides with the theoretical Figure 3 of Ref. [6].

5.2. *Waves in a cavity a with critically damped oscillating boundary*

Here, the motion of the boundary is no longer externally prescribed but driven by radiation pressure. A two-way coupling develops between the waves and the moving mirror, which renders theoretical predictions based on recurrence relations (33) much more challenging because ξ now depends on the entire history of $\mathscr{P}$. Thereafter, I focus on a specific limit in which this memory effect is restricted and can be explicitly accounted for: in addition to radiation pressure and linear restoring forces, the boundary is considered subject to critical damping, i.e., $F_{\text{ext}}=-2\alpha\dot{\xi}$. This dissipation makes the mirror relax on a timescale α that is assumed to be small compared with unity, that is, much faster than the time required for a pulse to travel back and forth in the cavity.

5.2.1. *Slow modulation of small-amplitude pulses*

The dynamics of the boundary are

$$\alpha^2\frac{\mathrm{d}}{\mathrm{d}t}\left(\gamma\dot{\xi}\right)=1-\xi-2\alpha\dot{\xi}+\mathscr{P}(t). \tag{36}$$

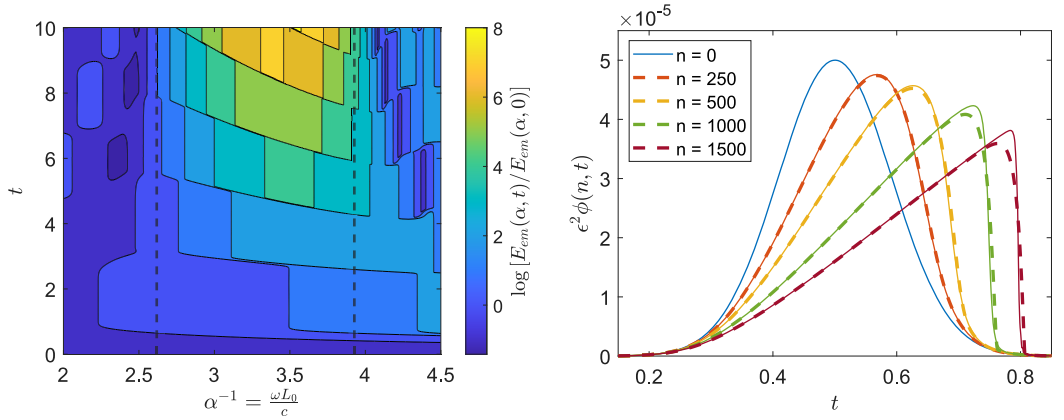

Figure 2. (Left) Energy E_{em} in a cavity of modulated length $\xi(t) = 1 + a\sin(\alpha^{-1}t)$. The initial conditions $u(x,0) = P(x,0) = \exp[-60(x-0.5)^2]$ and specific value of $a = 0.2$ are consistent with Ref. [6]. The dimensionless angular frequency $\alpha^{-1} = \omega L_0/c$ varies in increments of 0.01. The vertical dashed lines correspond to the theoretical instability range (35). (Right) Energy density at the left wall $\epsilon^2\phi(n,t) = u_L(t+2n)$ in a cavity whose right wall responds to the radiation pressure (n is the number of interactions between the pulse and the moving boundary). The initial conditions are $u(x,t) = -P(x,t) = \alpha^2\exp[-60(x-0.5)^2]$, $\xi(0) = 1$ and $\dot{\xi}(0) = 0$, with $\alpha = 5\times10^{-3}$. The dashed lines are the theoretical predictions of (42).

Assuming small-amplitude fields and a fast oscillator timescale α, which results in small displacements of the moving mirror, I expand

$$\mathscr{P}(t) = \epsilon^2 p(t), \quad \xi(t) = 1 + \epsilon^2\eta(t), \quad u_L(t) = \epsilon^2\varphi(t), \tag{37}$$

with $\alpha = \epsilon \ll 1$. Equation (36), at leading orders, models a fast critically damped oscillator,

$$\ddot{\eta} + \frac{2\dot{\eta}}{\epsilon} + \frac{\eta}{\epsilon^2} = p(t) + O(\epsilon^2), \tag{38}$$

the displacement of which is computed with a Green's function,

$$\eta(t) = \int_0^\infty s e^{-s/\epsilon} P(t-s)\,\mathrm{d}s = \int_0^\infty s e^{-s/\epsilon}\left[P(t) - s\dot{P}(t) + \cdots\right]\mathrm{d}s = P(t) - 2\epsilon\dot{P}(t) + O(\epsilon^2). \tag{39}$$

The recurrence relation (33) for $\mathscr{P}$ yields $p(t) = \varphi(t-1) + O(\epsilon^2)$ and the position of the mirror directly relates to the electromagnetic energy at the other end of the cavity some time before,

$$\eta(t) = \varphi(t-1) - 2\epsilon\dot{\varphi}(t-1) + O(\epsilon^2). \tag{40}$$

Equation (33) for u_L that connects two successive reflections of the pulse on the left wall becomes

$$\varphi\left[t + 1 + \epsilon^2\eta(t)\right] = \left[1 - 4\epsilon^2\dot{\eta}(t) + O(\epsilon^4)\right]\varphi\left[t - 1 - \epsilon^2\eta(t)\right]. \tag{41}$$

The successive bounces of a single pulse can be disentangled in this limit with $\phi(n,t) = \varphi(t+2n)$ with $t \in [0,2]$ and any integer n. This leads, with (40) and (41), to

$$\partial_n\phi + 6\epsilon^2\phi\partial_t\phi = 4\epsilon^3\left[(\partial_t\phi)^2 + 2\phi\partial_{tt}\phi\right] + O(\epsilon^4), \tag{42}$$

which is a regularized Burgers equation. At order ϵ^2, the total electromagnetic energy is conserved and it reduces to the strict Burgers equation, known to generate shock from any localized pulse [19]. Regularization and damping arise at the next order.

Consistent with (37), the simulations were initialized with $\xi(0) = 1$, $\dot{\xi}(0) = 0$ and $u(x,0) = -P(x,0) = \alpha^2\exp[-60(x-0.5)^2]$. The movie Movie3_alpha0p2 (Supplementary information)

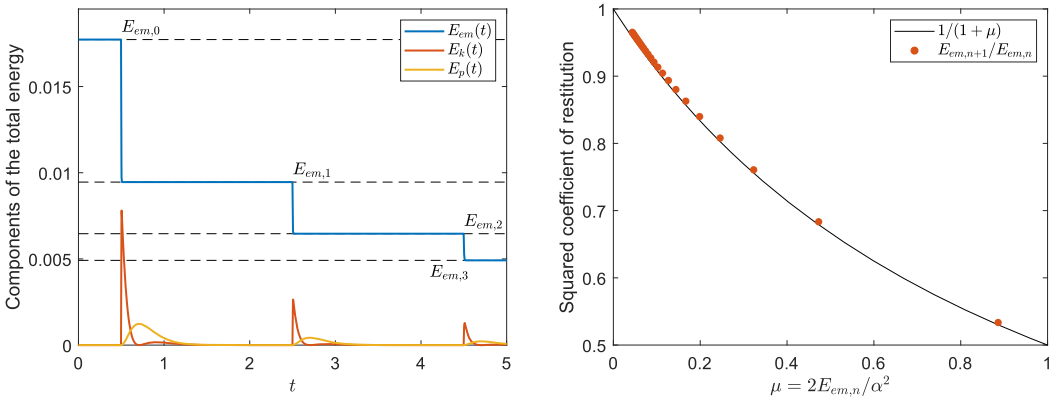

Figure 3. (Left) Energy in a cavity in which a pulse $u(x,0) = P(x,0) = 10\exp[-10^6(x-0.5)^2]$ interacts with a wall of a comparatively slow characteristic time. Rapid variations in the electromagnetic energy are observed, that can be modeled as shocks. (Right) Ratio of the final to initial electromagnetic energy for the first 25 shocks compared to (44).

illustrates the general dynamics and definition of the quantity of interest $\epsilon^2\phi(n,t) = u_L(t+2n)$ for $\alpha = 0.2$. However, this value of α is too large for (42) to hold. The results shown in Figure 2(right) for $\alpha = 5\times10^{-3}$ are in good agreement with the analysis derived in the limit of $\alpha \to 0$, except close to the peak of the pulse where comparatively fast dynamics occur that require higher order corrections.

5.3. *Shocks of very short pulses*

I now consider an initial condition with a pulse of very short duration compared to the response time of the critically damped oscillator. A similar formal analysis can be performed, that reveals that the radiation pressure is mainly balanced by inertia during these brief interactions. Conservation laws directly capture the electromagnetic energy loss during this shock, which is transferred to the mirror and eventually dissipated before the next interaction takes place.

Consider an electromagnetic pulse of dimensionless energy E_i and momentum $P_i = E_i$ traveling towards $x \to \infty$, that reflects off a comparatively slow oscillator initially at rest. Its final energy E_f corresponds to a momentum $P_f = -E_f$ because it then progresses towards $x \to -\infty$. The velocity of the mirror just after the pulse leaves is denoted as $\dot\xi_f$ (the position of the mirror is assumed to be unchanged). The conservation of energy and momentum are therefore

$$E_i = E_f + \alpha^2(\gamma_f - 1), \quad P_i = P_f + \alpha^2\gamma_f\dot\xi_f \Longrightarrow E_i = -E_f + \alpha^2\gamma_f\dot\xi_f, \tag{43}$$

where $\gamma_f = (1-\dot\xi_f^2)^{-1/2}$. This system can be solved for $\dot\xi_f$ and yields

$$\frac{E_f}{E_i} = \frac{1}{1+\mu}, \quad \gamma_f - 1 = \frac{\mu^2}{2+\mu}, \quad \mu = \frac{2E_i}{\alpha^2}. \tag{44}$$

The initial condition $u(x,0) = P(x,0) = 10\exp[-(x-0.5)^2/\sigma_x^2]$ and $\xi(0) = \dot\xi(0) = 0$ with $\sigma_x = 10^{-3}$ and $\alpha = 0.2$ illustrates this regime. Here, I refer the reader to the movie Movie4_sx0p001 (Supplementary information) that shows the dynamics up to $t = 5$. The various components of the energy are shown in Figure 3(left). The electromagnetic energy $E_{\rm em} = \int_0^\xi u(x,t)\,\mathrm{d}x$ is almost piece-wise constant (with values $\{E_{{\rm em},n}\}_n$), some of it being transferred as kinetic $E_{\rm k}(t) = \alpha^2\gamma(t)$ then potential $E_{\rm p}(t) = (\xi(t)-1)^2/2$ energies at each shock. The squared restitution coefficient E_f/E_i of (44) quantitatively compares to the DNS (see Figure 3(right)).

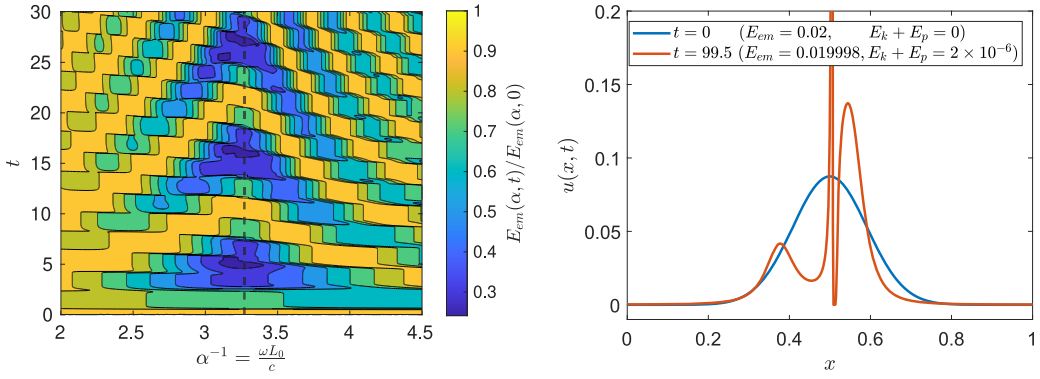

Figure 4. (Left) Energy E_{em} in a cavity whose left wall can oscillate with a natural angular frequency ω. The initial conditions $u(x,0) = P(x,0) = 0.02\sqrt{60/\pi}\exp[-60(x-0.5)^2]$ are similar to those of Figure 2(left). The dimensionless angular frequency $\alpha^{-1} = \omega L_0/c$ varies in increments of 0.01 and the vertical dashed line corresponds to $\alpha^{-1} = 3.27$. (Right) Energy density in the cavity at times $t = 0$ and $t = 99.5$ ($\alpha^{-1} = 3.27$).

6. Numerical simulations in the conservative limit

6.1. *Evolution of a single pulse*

The fully conservative regime, in which the moving boundary is only subject to the radiation pressure and a linear restoring force ($F_{\text{ext}} = 0$), represents a considerable theoretical challenge. In this section, I report numerical simulations that evidence the general dynamics, first considering the evolution of a single pulse of dimensionless energy 0.02 in a cavity initially at rest, i.e.,

$$u(x,0) = P(x,0) = 0.02\sqrt{\frac{60}{\pi}}\exp\left[-60(x-0.5)^2\right], \quad \xi(0) = 1, \quad \dot{\xi}(0) = 0. \tag{45}$$

Energy conservation implies that the displacement of the boundary is bounded, $|\xi(t) - 1| \leqslant 0.2$. The evolution of the electromagnetic energy for $\alpha^{-1} \in [2, 4.5]$ experiences periodic oscillations, as shown in Figure 4(left). For deeper insights, a longer run was computed for $\alpha^{-1} = 3.27$ of up to 100 time units: see movie Movie5_inva3p27 (Supplementary information) and Figure 4(right) that show the evolution of the initial and almost final electromagnetic energy $u(x,0)$ and $u(x,99.5)$. Although the pulse shapes develop sharp variations, the periodic evolution of the electromagnetic energy persists (it accounts for 99.99% of the total energy at $t = 99.5$). These slow recurrences are reminiscent of the Fermi–Pasta–Ulam–Tsingou (FPUT) problem in which the nonlinearity comes from the wave equation rather than coupling with a moving boundary, resulting in an extremely long time for thermal equilibrium to be reached [20].

6.2. *Equilibrium spectra*

As a more direct route to steady-state convergence, the numerical simulation is initialized with random electromagnetic noise in a cavity in which the moving boundary is at rest at time $t = 0$,

$$\tilde{u}_{n+1/2}(0) = E_{\text{em}}(0)\frac{\tilde{a}_{n+1/2}}{\sum_{m=0}^{N-1}\tilde{a}_{m+1/2}\Delta X}, \quad P(x,0) = 0, \quad \xi(0) = 1, \quad \dot{\xi}(0) = 0, \tag{46}$$

where $\{\tilde{a}_{n+1/2}\}$ are random values drawn from the uniform distribution on the open interval $(0,1)$ and $E_{\text{em}}(0)$ is the total energy in the system. The evolution of the spectral electromagnetic components in the cavity are difficult to compute using a spatial Fourier transform because the

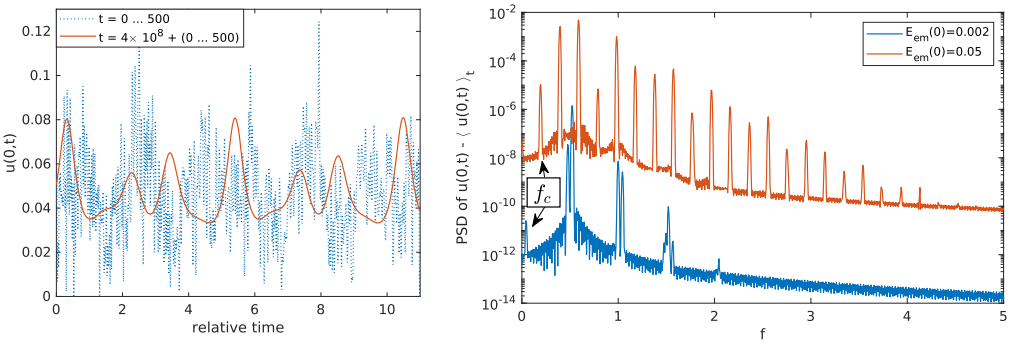

Figure 5. (Left) Energy density at the left (fixed) wall in a cavity initialized with random noise of total energy $E_{\rm em}(0) = 0.05$ with $N = 100$ grid points. (Right) PSDs of the energy density fluctuations at the left wall at final time $t \in [4\times10^8, 500 + 4\times10^8]$ for $E_{\rm em}(0) = \{0.002, 0.05\}$.

domain size evolves. A more convenient approach characterizes the temporal power spectrum density (PSD) of the energy density variations at the left (fixed) wall, $u(0,t) - \langle u(0,t)\rangle_t$ ($\langle\cdot\rangle_t$ denotes a time average over the range in which the PSD is computed). Simulations were run with $N = 100$ grid points, $\alpha^{-1} = \pi$, and three different values of $E_{\rm em}(0) = \{0.002, 0.01, 0.05\}$, up to 4×10^8 time units.

The supplemental movie Movie6_random_IC_N100_E0p05 depicts the dynamics at both the initial and final times for $E_{\rm em}(0) = 0.05$: the electromagnetic field clearly evolves toward a state that no longer displays high temporal or spatial frequencies. This is also evident from time series of $u(0,t)$ shown in Figure 5(left). This feature is observed in all three simulations. The PSDs at the final time are, for small values of the total energy $E_{\rm em}(0)$, almost restricted to the first eigenfrequencies of the linear system ($\{f_n = n/2\}_{n\geqslant1}$, see Figure 5(right)). As the total energy increases, the peak corresponding to $f_1 = 1/2$ splits in $f_1 \pm f_c/2$ because of nonlinear coupling with the moving boundary: the very low frequency f_c, also observed in the PSDs, is found to slowly modulate the oscillation amplitude of $\xi(t)$ and to scale with the total energy as $f_c = 3.8E_{\rm em}$. This relation has been confirmed for a larger number of grid points N ($N = 200$ and $E_{\rm em} = 0.05$). Even though the extinction of the high frequencies may be caused by numerical dispersion, these results nevertheless support the possibility of nonlinear steady states with very simple spectral structures in which the waves are strongly coupled with the motion of the moving boundary.

7. Conclusion

The two-way coupling between linear waves trapped in a cavity and a fast moving boundary undergoing large displacements was introduced in the context of classical electromagnetism. No practical experimental setup can follow this model because it involves perfect mirrors moving at a fraction of the speed of light (the only plausible relevance is in astrophysics, at the surface of highly conductive neutron stars [21]). However, it provides a convenient framework to evidence emerging features such as the generation of sharp profiles Section 5.2.1, finite restitution coefficients for fast waves Section 5.3, slow recurrences Section 6.1, nonlinear steady-states in which energy is concentrated in a few modes Section 6.2. These observations can guide the understanding of experiments with mechanical waves, such as water waves generated by a paddle in a container or acoustic waves forced by a piezoelectric device in a cavity. It shows that qualitative behavior usually ascribed to the bulk non-linearities can also result from a *linear* propagation coupled with a moving boundary.

Declaration of interests

The authors do not work for, advise, own shares in, or receive funds from any organization that could benefit from this article, and have declared no affiliations other than their research organizations.

Supplementary data

Supporting information for this article is available on the journal's website under https://doi.org/10.5802/crphys.242 or from the author.

References

[1] G. Goedecke, V. Toussaint and C. Cooper, "On energy transfers in reflection of light by a moving mirror", *Am. J. Phys.* **80** (2012), pp. 684–687.
[2] D. Censor, "The generalized Doppler effect and applications", *J. Franklin Inst.* **295** (1973), pp. 103–116.
[3] D. Censor, "Acoustical Doppler effect analysis–Is it a valid method?", *J. Acoust. Soc. Am.* **83** (1988), pp. 1223–1230.
[4] N. Mujica, R. Wunenburger and S. Fauve, "Scattering of a sound wave by a vibrating surface", *Eur. Phys. J. B* **33** (2003), pp. 209–213.
[5] G. Michel, "The generalized Doppler effect for surface waves", *Europhys. Lett.* **116** (2016), article no. 44002.
[6] J. Dittrich, P. Duclos and P. Šeba, "Resonance response of the quantum vacuum to an oscillating boundary", *Phys. Rev. E* **49** (1994), pp. 3535–3538.
[7] O. Méplan and C. Gignoux, "Exponential growth of the energy of a wave in a 1D vibrating cavity: application to the quantum vacuum", *Phys. Rev. Lett.* **76** (1996), pp. 408–410.
[8] V. V. Dodonov, "Nonstationary Casimir effect and analytical solutions for quantum fields in cavities with moving boundaries", *Phys. Scr.* **82** (2010), article no. 038105.
[9] J. Cooper, "Long-time behavior and energy growth for electromagnetic waves reflected by a moving boundary", *IEEE Trans. Antennas Propag.* **41** (1993), pp. 1365–1370.
[10] M. Aspelmeyer, T. J. Kippenberg and F. Marquardt, "Cavity optomechanics", *Rev. Mod. Phys.* **86** (2014), pp. 1391–1452.
[11] S. Barzanjeh, A. Xuereb, S. Gröblacher, M. Paternostro, C. A. Regal and E. M. Weig, "Optomechanics for quantum technologies", *Nat. Phys.* **18** (2022), pp. 15–24.
[12] V. V. Dodonov, "Fifty years of the dynamical Casimir effect", *Physics* **2** (2020), no. 1, pp. 67–104.
[13] C. K. Law, "Interaction between a moving mirror and radiation pressure: a Hamiltonian formulation", *Phys. Rev. A* **51** (1995), no. 3, pp. 2537–2541.
[14] S. Butera and I. Carusotto, "Mechanical backreaction effect of the dynamical Casimir emission", *Phys. Rev. A* **99** (2019), article no. 053815.
[15] L.-L. Nian and J.-T. Lü, "Heat transfer mediated by the dynamical Casimir effect in an optomechanical system", *Phys. Rev. A* **103** (2021), article no. 063510.
[16] O. Di Stefano, A. Settineri, V. Macrì, A. Ridolfo, R. Stassi, A. F. Kockum, S. Savasta and F. Nori, "Interaction of mechanical oscillators mediated by the exchange of virtual photon pairs", *Phys. Rev. Lett.* **122** (2019), article no. 030402.
[17] F. Harfoush, A. Taflove and G. A. Kriegsmann, "A numerical technique for analyzing electromagnetic wave scattering from moving surfaces in one and two dimensions", *IEEE Trans. Antennas Propag.* **37** (1989), pp. 55–63.
[18] T. T. Koutserimpas and C. Valagiannopoulos, "Electromagnetic fields between moving mirrors: singular waveforms inside Doppler cavities", *Opt. Express* **31** (2023), pp. 5087–5101.
[19] G. B. Whitham, *Linear and Nonlinear Waves*, John Wiley & Sons: New York, 2011.
[20] N. J. Zabusky and M. D. Kruskal, "Interaction of "solitons" in a collisonless plasma and the recurrence of initial states", *Phys. Rev. Lett.* **15** (1965), no. 6, pp. 240–243.
[21] G. Baym, C. Pethick and D. Pines, "Electrical conductivity of neutron star matter", *Nature* **224** (1969), pp. 674–675.